T2R2 東京工業大学リサーチリポジトリ
Tokyo Tech Research Repository

論文 / 著書情報
Article / Book Information

Title	Development of Giacometti Arm With Balloon Body
Authors	Masashi Takeichi, Koichi Suzumori, Gen Endo, Hiroyuki Nabae
Citation	IEEE Robotics and Automation Letters (RAL), Vol. 2, Issue 2, pp. 951-957
Pub. date	2017, 1
Copyright	(c) 2017 IEEE. Personal use of this material is permitted. Permission from IEEE must be obtained for all other uses, in any current or future media, including reprinting/republishing this material for advertising or promotional purposes, creating new collective works, for resale or redistribution to servers or lists, or reuse of any copyrighted component of this work in other works.
DOI	https://dx.doi.org/10.1109/LRA.2017.2655111
Note	This file is author (final) version.

Powered by T2R2 (Tokyo Institute Research Repository)

Development of Giacometti Arm with Balloon Body*

Masashi Takeichi, Koichi Suzumori, *Member, IEEE*, Gen Endo, *Member, IEEE*, and Hiroyuki Nabae, *Member, IEEE*

***Abstract*— As part of our research on developing different types of Giacometti robots, the potential of a very long, very light, and very simple robot arm with a balloon body is discussed in this paper. Although this robot arm is not suitable for precise positioning, rapid motion, and high load capacity, which are the aspects most conventional robots focus on, it is designed for very specific purposes such as inspection using a small camera at its tip and is designed to be essentially safe even if it falls down or hits an object. This robot arm is realized using helium-filled balloon bodies and thin pneumatic muscles. The arm achieves self-weight compensation, and the possibility of designing a very long arm is confirmed theoretically and experimentally. A prototype of a 7-m-long cantilever arm is designed, developed, and tested.**

I. Introduction

Currently, many types of robots are being developed. Most of them consist of rigid linkage mechanisms driven by motors. Although such robots exhibit high performance and have many functions, they are usually heavy and have complicated systems, which sometimes make them difficult to handle and dangerous when control is lost. Consequently, it is sometimes difficult to put such robots to practical use.

We have proposed "Giacometti robotics" as a new robotics concept, whose idea is opposite to that of most conventional robots, which focus on high speed, precise positioning, and high load capacity [1]. Giacometti robotics was named as such by our team after Alberto Giacometti, who was a Swiss sculptor. Giacometti robotics aims to realize robots that are very light and very simple, easy to handle, and essentially safe by focusing on an essential function and ignoring the other functions. This new concept matches the characteristics of Giacometti sculptures, which are very thin and simple without flesh. We believe that Giacometti robots have the potential to be adopted rapidly for field operations because they are very lightweight and essentially safe. Examples of Giacometti robots include walking robots with very light bodies that can climb on rubble in disaster areas or walk on vertical surfaces and very long robot arms that can perform inspections in disaster areas. They are essentially safe even if they fall down because they are very light. We have already developed the Hexapod Giacometti Robot [2], which has very long, light, and thin legs, and have demonstrated its huge potential. In this paper, we discuss the potential of a long robot arm called the "Giacometti Arm with Balloon Body", particularly in the feasibility of inspection. The robot is expected to be used for search and inspection during the early stage of disasters.

Previous works on robots with very long arms include the Articulated Inspection Arm of CEA, France [3] and the Snake-arm Robot of OC Robotics [4]. These robots exhibit high performance and can work in hazardous environments, but they consume very high power and need careful control. If these robots lose control and fall down, the robots and their environment will suffer heavy damage because their bodies are heavy and stiff. To avoid such danger, some studies have investigated the use of inflatable structures. Inflatable bodies are very safe for use around people because they are very light and soft [5,6]. The concept of the inflatable robotic arm [7,8] is the closest to the idea of the Giacometti robot proposed in this paper. In a previous work, a 3-m-long inflatable arm with three degrees of freedom (DOFs) was driven by a tendon [9]. This arm weighs 500 g, can carry a 600-g payload, and has approximately ±80° of movable range. If the robot is designed to be longer, the transfer of wire force at the tip joints might become difficult. Increasing the arm length has a major impact on reaching more distant locations. A drone is also useful for inspection during the early stage of disasters. However, it requires many serious safety considerations before being introduced into an area. It often encounters many physical obstacles and radio contact issues. It is difficult to perform careful inspections because the flight time is limited. There are some helium-filled robots such as the Air_ray [10] and AirPenguins [11], but their bodies have to be large in order to lift their conventional motors and batteries. Therefore, they cannot be used in applications where space is limited.

Therefore, we develop a robot arm that is light, safe, and long. Two key components help us to realize these requirements: a thin McKibben artificial muscle actuator developed in our laboratory [12], and helium-filled inflatable balloons that compensate for self-weight. The characteristics of these components are described in section II. Our goal is to develop a very light and long (20 m) robot arm having 20 DOFs that can be used for inspections in disaster sites. As the first step toward this goal, we have developed a 7-m-long robot arm with seven joints and seven DOFs. An image of the Giacometti Arm with Balloon Body is shown in Fig. 1.

*This work is supported by MEXT KAKENHI (Grant Number: 15K13907) under the project "Experimental Proof of Giacometti Robotics Potential".

Masashi Takeichi is with the Department of Mechanical Engineering, Tokyo Institute of Technology, 2-12-1 Ookayama, Meguro-ku, Tokyo 152-8552, Japan (e-mail: takeichi.m.aa@m.titech.ac.jp).

Koichi Suzumori is with the Graduate major in Mechanical Engineering, Tokyo Institute of Technology, (e-mail: suzumori@mes.titech.ac.jp).

Gen Endo is with the Graduate major in Mechanical Engineering, Tokyo Institute of Technology, (e-mail: gendo@mes.titech.ac.jp).

Hiroyuki Nabae is with the Graduate major in Mechanical Engineering, Tokyo Institute of Technology, (e-mail: nabae@mes.titech.ac.jp).

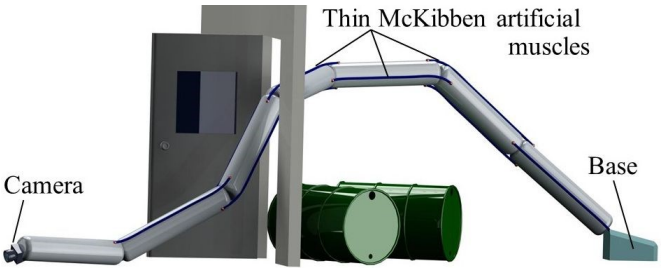

Figure 1. Schematic design of Giacometti Arm with Balloon Body. The arm is very long and light and is safe for use around people because of its compliance and lightness.

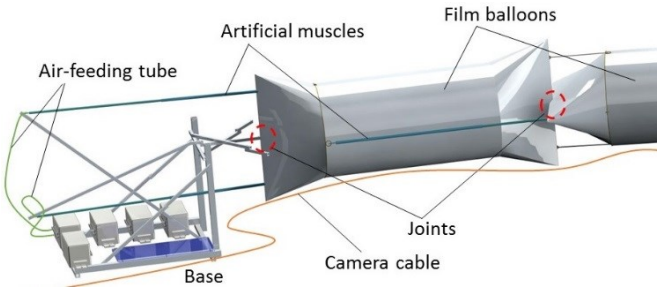

Figure 2. Schematic of arm around base. The base is equipped with analog valves, a microcomputer, and a control switch for the arm. The joints are connected by a wire.

II. Schematic Design

A. Over view

The schematics of the arm around the base is shown in Fig. 2. The arm consists of helium-gas-filled polyethylene balloons (link structures), thin McKibben artificial muscles, thin air-feeding tubes, a small camera at the robot arm tip, and cables for the camera. The application of pressure to each artificial muscle drives the arm. For example, the arm can be made to move in the upward direction by shrinking the upper-side artificial muscle through applied pressure and expanding the lower-side artificial muscle through decompression.

Inflatable balloons are filled with helium gas to compensate for their self-weight. The combination of thin McKibben artificial muscles and inflatable structures has the following merits.

- The actuator and air tubes that drive it weigh only several grams per meter, and the buoyancy of one link is approximately 30 g/m. Therefore, the robot arm achieves full self-weight compensation at each link, which enables a very long cantilever-type robot arm to be realized.
- Tendon-driven robot arms with motors mounted on the robot base might be another design option to realize a very long arm. However, tendon-driven arms need arm structures with high stiffness to resist the tendon force and hence avoid buckling, or the base-side arm structure must resist the tendon reaction force, which drives robot joints located in the upper side. In contrast, the thin McKibben artificial muscles generate forces only between connected links. This makes it possible for inflatable materials with low rigidity to work as robot arms.

We design an arm that can carry a CMOS camera (CP-100B, YKmusen, Japan, body weight: 3 g, Number of pixels: 300,000 pixels) at the tip. Though the arm does not work precisely or rapidly, it continues working even if it hits objects such as walls and floors and is safe even if it falls down because the robot has high compliance and hardly causes any damage owing to its softness and lightness.

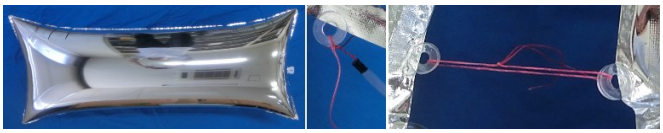

Figure 3. One complete balloon (left), bonding of balloon and thin artificial muscle (center), and two links connected by wire (right).

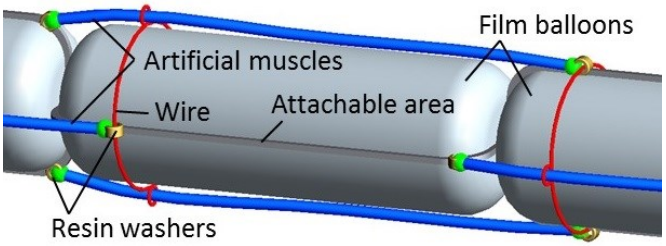

Figure 4. Schematic of surrounding area of joint. An attachable area and a connection-prohibited area exist in the film balloon. We use only the attachable area for connections. The rolling motion is controlled by the red wire. The wires connecting two balloons inhibit the translation of the muscles in the circular direction of the balloon.

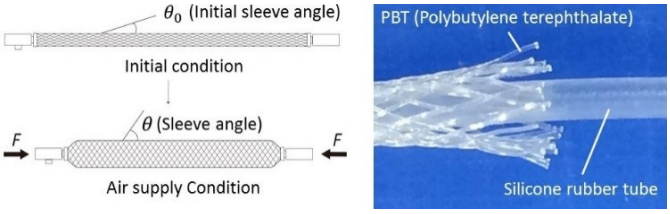

Figure 5. Thin McKibben artificial muscles driven by pneumatics: full schematic (left) and close-up view (right). The tube diameter is 1.3 mm.

B. Inflatable Balloon

Each film balloon is 1 m in length and 0.3 m in diameter (Fig. 3). The film balloons consist of a three-layer structure: aluminized film, nylon film, and polyethylene film. The aluminized films strengthen the balloon structure and prevent helium leakage. To lighten the weight, the balloons are serially connected using resin wires (Dyneema®) (Fig. 3). These connections work as robot joints. The balloon has an attachable area where the double films are welded together. To facilitate the tying of thin artificial muscles and wires used for connecting two balloons, small resin washers are bonded to the connecting area (Fig. 3). The rolling motion of a joint is inhibited by preventing artificial muscle translation in the circular direction of the balloon using the wire (Fig. 4).

C. Thin Artificial Muscle

We use thin McKibben artificial muscles developed in our laboratory [12, 13] (Fig. 5) as actuators that are pneumatically driven and have a much bigger output force-to-weight ratio than conventional actuators. Table 1 compares the characteristics of the developed thin muscle and a commercially available one (FESTO DMSP-5).

TABLE I. COMPARISON OF THIN ARTIFICIAL MUSCLE AND COMMERCIAL ONE (FESTO DMSP-5).

	Thin artificial muscle used in our robot	Commercially available muscle [FESTO]	Unit
Diameter	1.8	5.0	[mm]
Weight	1	27	[g/m]
Maximum shrink ratio	26	20	[%]
Maximum shrink force	14	49	[N]
Output force/weight	14	1.8	[N/g]

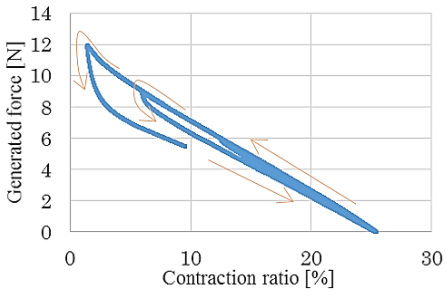

Figure 6. Relationship between contraction ratio and generated force when pressure is 0.3 MPa. The experiments are reciprocated from 0 to 6 N, 0 to 9 N, and 0 to 12 N in generated force.

III. MODELING AND DESIGN

To develop the Giacometti Arm with Balloon Body, models of the thin artificial muscle (subsection A) and arm joint (subsection C) are required for design and control. Subsection B discusses the arm statics based on the model described therein. In addition, the effect of increasing the arm length is discussed in subsection D.

A. Thin Artificial Muscle Statics

The basic characteristics of the thin McKibben artificial muscles are discussed in this subsection. The muscles have three parameters: air supply pressure, generated force, and contraction ratio. To construct the geometric and static models of the arm, the relationship between these parameters should be formulized. We investigate the static characteristics by measuring the relationship between the generated force and contraction ratio under various pressure levels.

We experimentally obtain the static characteristics of the artificial muscles while changing the pressure and artificial muscle length in a quasi-static manner. The artificial muscles have nonlinear characteristics, but this nonlinearity is found only around the high-pressure area and the area close to the original length (Fig. 6). For simple formulation, we use the linear region of the curve in Fig. 6 and approximate the relationship between the contraction ratio and force by a straight line (Fig. 7). The relationship is expressed as

$$\frac{\varepsilon}{b}+\frac{f}{a}=1 \quad (1)$$

where ε and f are the contraction ratio and generated force, respectively. The values of a and b are given by the f and ε intercepts of the approximated curve. Fig. 8 shows the values of a and b obtained from the experimental results. From this experimentally obtained equation, we can obtain one of the three values (contraction ratio, generated force, or pressure) when the values of the other two parameters are known.

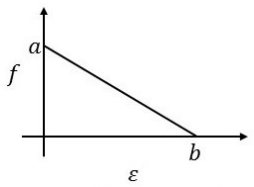

Figure 7. Model of relationship between contraction ratio and generated force approximated to straight line.

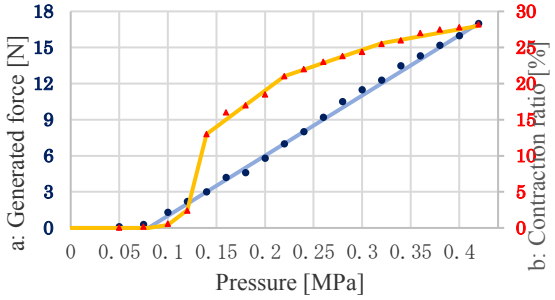

Figure 8. Variation of parameters a and b according to pressure.

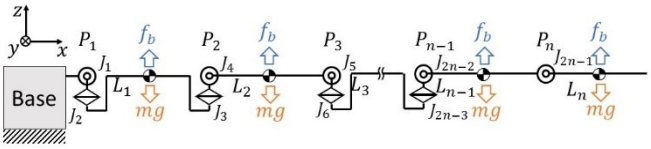

Figure 9. Modeling of robot arm. L_k, P_k, and J_k denote the k-th link, coordinate of the k-th joint, and k-th joint having one DOF, respectively.

B. Arm Statics

The arm is modeled as shown in Fig. 9. It seems to have two DOFs at each point, but its actuators, except the one at the base, cross over two joints to expand the moving range. Thus, the DOFs are actually half because the two joints are synchronized with each other. For example, J_2 and J_3 show synchronized motion.

The moment for each joint is calculated to determine the diameter of balloon bodies from the perspective of self-weight compensation. The tip link is regarded as the n-th link; the moment is given by

$$M_{all}=\frac{nl}{2}\left[\{n(m_m+m_l+m_j)-m_j\}g-nf_b\right]+nlm_cg$$
$$+\sum_{k=1}^{n}\left(k-\frac{3}{2}\right)la_km_pg+\sum_{k=1}^{n}2(n-k)\left(k-\frac{1}{2}\right)lm_tg \quad (2)$$

where l, m_m, and r represent the length, mass, and radius of the film balloon, respectively. m_p is the mass of the artificial muscle. a_i indicates the required number of artificial muscles for moving the i-th link. m_t and m_l represent the masses of the air-feeding tube and camera cables per unit length. m_c and m_j represent the masses of the camera and joint parts. f_b shows the buoyancy of the helium-filled balloon per unit volume. The unit length and volume indicate the length and volume of one link. The mass of the film balloon is relative to its radius, and the buoyancy is proportional to the square of its radius. The radius plays a very important role in achieving self-weight compensation. A comparison of the weight of each link indicates that the arm that is closest to the base is the heaviest link because it has the largest number of air-feeding tubes. Considering the balance of the weight and

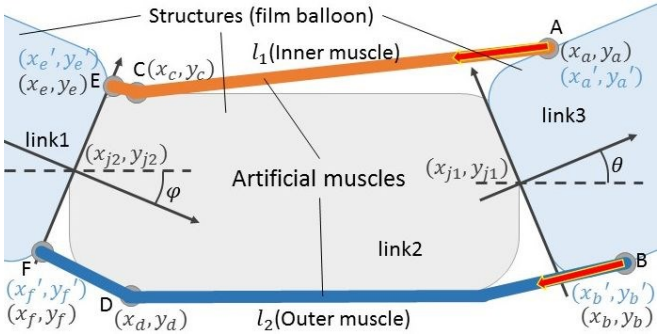

Figure 10. Analytical model of joint configuration. The length of the artificial muscles affect the range of the bending angle.

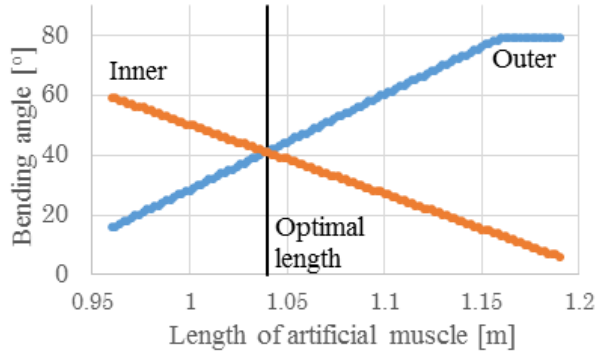

Figure 11. Allowable bending angles ($\rho E\theta$) of arm considering length of inner (red line) and outer (blue line) artificial muscles.

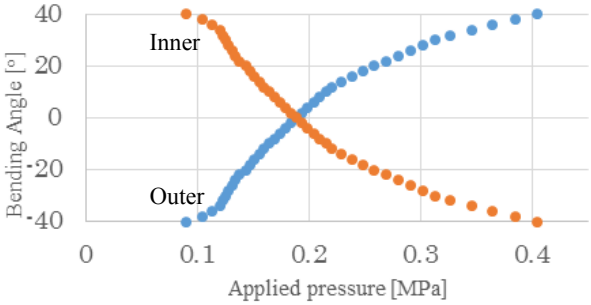

Figure 12. Relationship between applied pressure and bending angle ($\rho E\theta$) of two joints.

buoyancy of the arm, the following equation is obtained:

$$f_b \frac{l_n {r_1}^2}{lr^2} = \left(m_m \frac{l_n r_1}{lr} + 38m_t' + m_l' + m_j + 2m_p\right) g \quad (3)$$

where $m_t' = m_t l_n / l, m_l' = m_l l_n / l$. From this equation, we obtain $r_1 \geq 114.8$ mm by substituting specific parameters to guarantee sufficient buoyancy. In this paper, we use a 300-mm-diameter film balloon to guarantee sufficient buoyancy for self-weight compensation.

C. Joint Statics

The joint model is shown in Fig. 10. The shorter the artificial muscle length, the shorter is the maximum of l_2 and the smaller is the bending angle. On the other hand, if the length is large, l_1 is not sufficient to ensure shrinking and the bending angle becomes small. However, the artificial muscles on both sides should have the same initial length. These facts indicate the existence of a trade-off problem wherein a short artificial muscle is suitable for ensuring shrinking but it interferes with the bending motion when it is not on the shrinking side. Therefore, we optimize the length of the artificial muscle so that the movable range of the joint becomes maximum. At this point, the bending angle is denoted by $\rho E\theta$ in Fig. 10. The allowable angle can be chosen as the smaller of the two maximum angles obtained from the shrinking length of the inner artificial muscle (l_1 in Fig. 10) and from the initial length of the outer artificial muscle (l_2 in Fig. 10), as shown in Fig. 11. The range of muscle lengths shown in Fig. 11 corresponds to the lengths required to apply a pressure of 0 to 0.4 MPa. Then, the optimal initial length (1.04 m) of the muscle is obtained. From these results, the contraction ratio and generating force can be calculated according to the joint angle. The bending is fixed by antagonistic moments of 0.3 Nm generated by the inner and outer muscles. The contraction ratio and generating force are determined based on the bending angle (Fig. 10), and the required pressure for each artificial muscle can be obtained based on the data presented in section III. A. The required pressure according to the angle is shown in Fig. 12.

D. Thin Artificial Muscle Statics

If self-weight compensation can be achieved sufficiently by buoyancy, the arm can be extended infinitely. However, the problems of large inertia and responsiveness of the artificial muscles strongly affect the motion of the arm. Thus, we investigate the effect of these two parameters on the dynamics of the arm. This calculation indicates the possibility of a 20-m-long robot arm.

First, a simple Giacometti Arm model considering inertia and air resistance is constructed using Simulink (The MathWorks, Inc.). The bodies are approximated by cylinders. A pair of thin artificial muscles is attached to the base link position, and the pair can change the spring constant and initial length according to the air supply pressure (Fig. 13). The equation of motion is given by

$$I\ddot{\theta} + M_C + M_A + M_B = 0 \quad (4)$$

where M_c represents the moment generated by air resistance and M_a and M_b represent the moments generated by the upper and lower artificial muscles, respectively.

$$M_C = \int x \cdot dF_D = \frac{\rho}{8} C_D \cdot 2r \cdot (nl)^4 \cdot \dot{\theta}^2 \quad (5)$$

where

$$dF_D = C_D \frac{\rho}{2} \left(x\dot{\theta}\right)^2 dA \quad (6)$$

Here, dF_D represents the air resistance in the cross section dA. C_D, ρ, and $x\dot{\theta}$ indicate the drag coefficient, fluid density, and the speed at x (length from the origin), respectively. As shown in Fig. 14, 120 s are required to produce the maximum stroke of the arm when n is 20. The simulation shows that no oscillation affects the inspection because the damping due to the air resistance is predominant owing to the fact that the Giacometti Arm is very light and soft.

Second, we investigate the effect of the response time of the thin artificial muscles when the length of the air-feeding tubes (PFA microtube) increases. The tube length depends on the arm length. We express the response time as

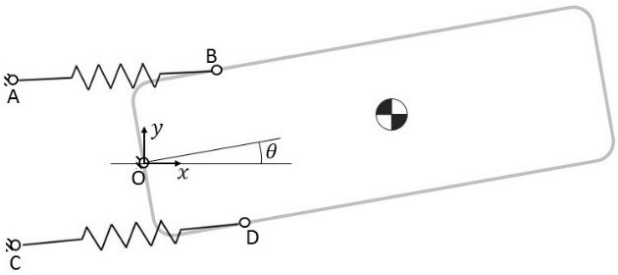

Figure 13. Model of relationship between contraction ratio and generated force approximated to straight line.

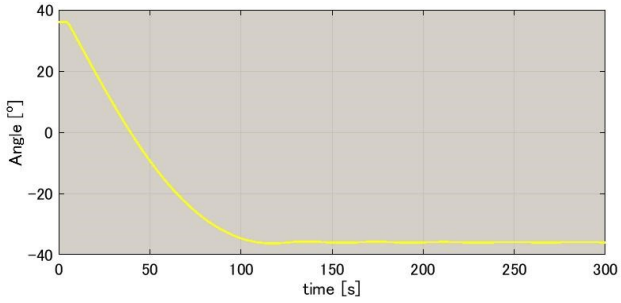

Figure 14. Step response of long arm obtained by numerical simulation (n = 20)

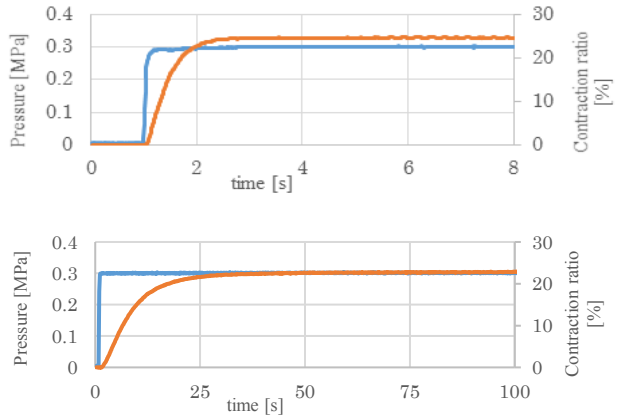

Figure 15. Step response of artificial muscle when step response of 0.3 MPa is given. The blue line shows the pressure according to the left scale, and the orange line shows the contraction ratio of the artificial muscle according to right scale. The tube length is 0.1 and 10 m in the upper and lower figures, respectively.

$$t(l) = t_0 + F(l) \tag{7}$$

Here, t_0 represents the delay at the connector between the valve and microtube. $F(l)$ indicates the delay incurred by the microtube, according tube length l.

We obtained $F(l)$ experimentally because it is difficult to calculate analytically. The response time of the artificial muscle is obtained when a step input of 0.3 MPa is applied. Fig. 15 shows the step responses of the artificial muscles, and Fig. 16 shows the relationship between the tube length and 95% injection time. $F(l)$ can be approximated linearly, and we can estimate that the response time is less than 1 min when the arm length is 20 m.

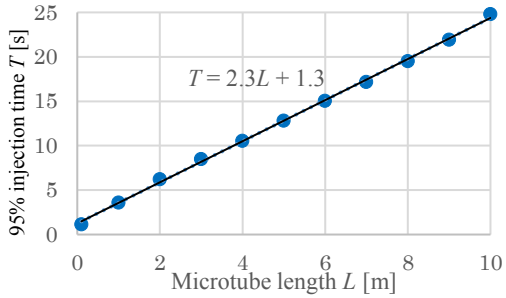

Figure 16. Relationship between tube length and 95% injection time of artificial muscle. The equation represents the approximated line.

Figure 17. Complete three-link arm.

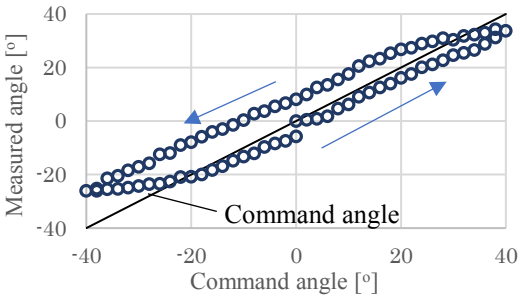

Figure 18. Comparison of measured angle between first and third links with command angle.

IV. Experiment

A. Experiment with Three-link Arm

The First, a three-link arm is developed (Fig. 17) to verify the concept described in section III. The balloon diameter and artificial muscle length are decided based on the discussion in III-B and III-C. The three-link arm has 3 DOFs and is driven by 6 thin artificial muscles. The pneumatic pressure given to each muscle is controlled by using an analog pressure control regulator, which is driven according to the pulse-width-modulated signal of the command angle from a microcomputer. The developed arm has no sensors and is controlled manually as an open loop system. The actual angle between the first and third links, obtained from the side view movie, is compared with the command angle in Fig. 18. The arm motions during the experiments are shown in Fig. 19 with time stamps. The reasons for the error between the actual and desired motions found in Fig. 18 are as follows: (1) The actual behavior cannot be simulated well through modeling. (2) The weight and buoyancy do not balance well. (3) The interference between balloons becomes high as the join angle is increased.

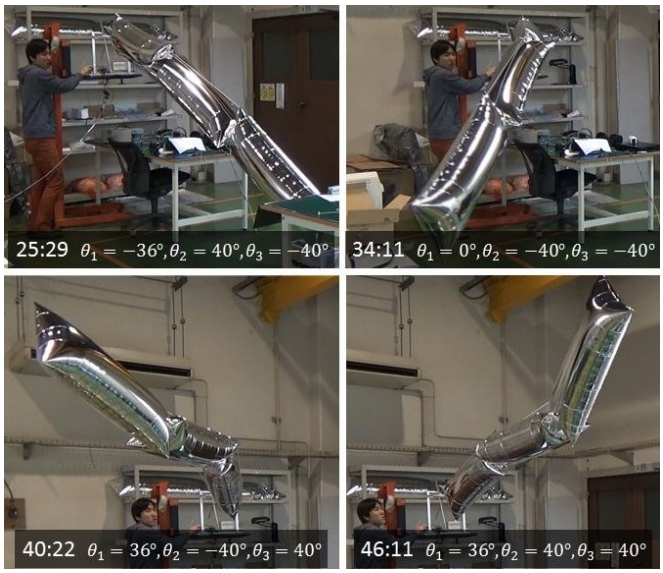

Figure 19. Actual motion of three-link arm. (The captions show the elapsed time and each command angle. θ_1, θ_2, and θ_3 represent J_1, $J_2 + J_3$, and $J_4 + J_5$ in Figure 9.)

TABLE II. SPECIFICATIONS OF SEVEN-LINK ARM COMPARED WITH INFLATABLE ARM [9]

	Length	Diameter	Weight	Movable angle	Payload
Seven-link arm	7 [m]	0.3 [m]	340 [g]	±30 [°]	20 [g]
Inflatable arm [9]	3 [m]	0.2 [m]	500 [g]	±80 [°]	500 [g]

B. Experiment with Seven-link Arm

The results for the three-link arm are extended to a seven-link arm. We control 7 joints using the control method discussed in III-C. Further, we mount a tiny camera at the arm tip to obtain the view from the tip. The specifications of the seven-link arm are listed and compared with the inflatable arm [9] in Table 2. Although the seven-link arm's movable angle and payload are smaller than those over the inflatable arm [9], it shows length and weight superiority of seven-link arm. The motion of the arm is shown in Fig. 20 with time stamps. Based on visual images from the camera, we confirm that the arm movement is sufficiently smooth to track a target or human controlled by heuristically visual feedback, as shown in each of the upper-left pictures in Fig. 20. We also confirm that the response time of the base joint is 21 s, which has the biggest momentum inertia for end-to-end movement (joint angles from +36° to -36°). Because the response time is 16 s at $n = 7$ according to the Simulink simulation results presented in section III. D, we verify that the simulation is useful.

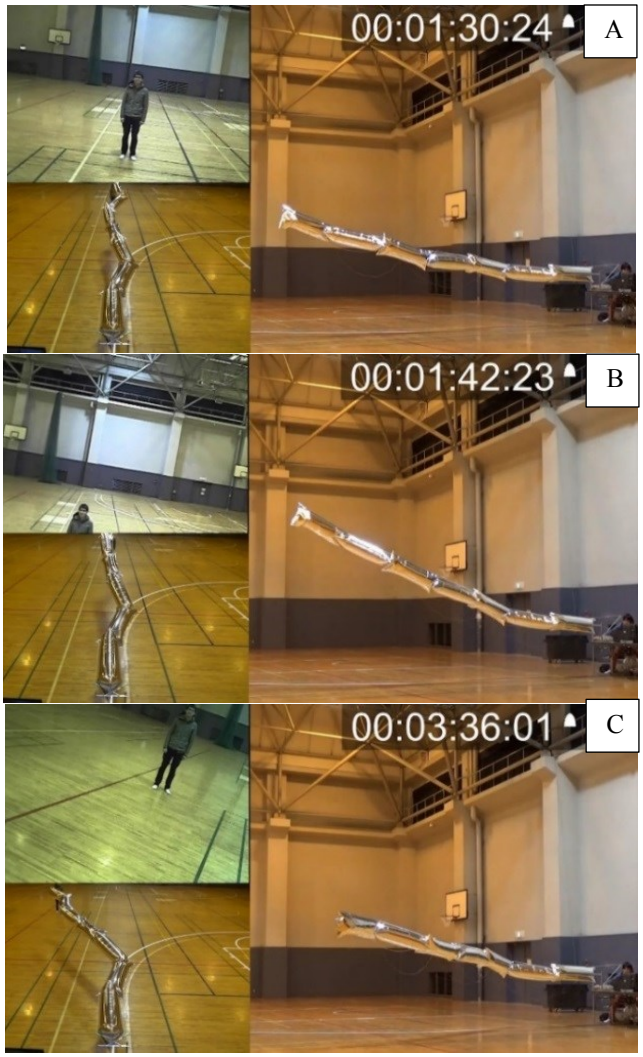

Figure 20. Arm motions (upper left: view from camera mounted on arm tip, lower left: view from robot base, right: complete view of arm).

V. CONCLUSION

We have designed and developed a seven-link Giacometti robot arm with a balloon body. The prototype is 7 m in length and works well. Its weight is only 340 g. Although the arm does not have good load capacity, positioning preciseness, or speed, it is essentially safe even if it falls down or goes out of control because of its lightness and softness. We believe that the prototype experimentally confirms the great potential of Giacometti robotics as a new robotics discipline.

The characteristics of the Giacometti Arm with Balloon Body are analyzed theoretically. A theoretical model for design and control is developed, and the model results are compared with experimental results obtained using a three-link prototype. We confirm that they roughly agree although the objective of the range of movement is not met. Further, the possibility of creating a 20 m Giacometti Arm with a camera is confirmed theoretically.

We will evaluate the detail characteristics related to accuracy, payload, and stiffness and will construct a control system based on them in our subsequent studies.

REFERENCES

[1] K. Suzumori, "New pneumatic artificial muscle realizing Giacometti robotics and soft robotics," in *6th Int. Conf. Manufacturing, Machine Design and Tribology (ICMDT 2015)*, Okinawa, Japan, 2015, pp. 4–5.

[2] S. Kurumaya, F. Ni, and K. Suzumori, "Design of hexapod Giacometti robot with very long, light, and thin legs," in *Proc. 6th Int. Conf. Advanced Mechatronics (ICAM2015)*, Tokyo, Japan, 2015, pp. 136–137.

[3] Y. Perrot, J. J. Cordier, J. P. Friconneau, L. Gargiulo, E. Martin, J. D. Palmer, and A. Tesini, "ITER articulated inspection arm (AIA): R&d progress on vacuum and temperature technology for remote handling," *Fusion Eng. Des.*, vol. 75–79, pp. 537–541, Nov. 2005.

[4] OC Robotics [Online], Available: http://www.ocrobotics.com/, Accessed on: Feb. 29, 2016.

[5] S. Sanan, M. H. Ornstein, and C. G. Atkeson, "Physical human interaction for an inflatable manipulator," in *33rd Annu. Int. Conf. IEEE EMBS*, Boston, Massachusetts, USA, 2011, pp. 7401–7404.

[6] R. Qi, T. L. Lam, and Y. Xu, "Mechanical design and implementation of a soft inflatable robot arm for safe human-robot interaction," in *IEEE Int. Conf. Robotics & Automation (ICRA)*, Hong Kong, China, 2014, pp. 3490–3495.

[7] S. Voisembert, A. Riwan, N. Mechbal, and A. Barraco, "A novel inflatable robot with constant and continuous volume," in *IEEE Int. Conf. Robotics and Automation*, Shanghai, China, 2011, pp. 5843–5848.

[8] S. Voisembert, N. Mechbal, A. Riwan, and A. Aoussat, "Design of a novel long-range inflatable robotic arm: Manufacturing and numerical evaluation of the joints and actuation," *J. Mech. Robotics*, vol. 5, pp. 045001, 2013.

[9] Robotics in Video [Online], Available: http://derobotica.blogspot.jp/ 2013/01/long-range-inflatable-robot-arm.html#.V7vewPntlBc, Accessed on: Aug. 23, 2016.

[10] Air_ray | Festo Corporate [Online], Available: https://www.festo.com/ group/en/cms/10245.htm, Accessed on: Dec. 2, 2016.

[11] AirPenguins | Festo Corporate [Online], Available: https://www.festo. com/group/en/cms/10242.htm, Accessed on: Dec. 2, 2016.

[12] M. Takaoka, K. Suzumori, S. Wakimoto, K. Iijima, and T. Tokumiya, "Fabrication of thin McKibben artificial muscles with various design parameters and their experimental evaluations," in *5th Int. Conf. Manufacturing, Machine Design and Tribology (ICMDT 2013)*, Busan, South Korea, 2013, p. 82.

[13] S. Kurumaya, K. Suzumori, H. Nabae, and S. Wakimoto, "Musculoskeletal lower‐limb robot driven by multifilament muscles," Robomech Journal, Springer Open, 3:18, Sep. 2016.